

Neuroglia Infection by RABV after Anterograde Virus Spread in Peripheral Neurons

Madlin Potratz, Luca M. Zaack, Carlotta Weigel, Antonia Klein, Conrad M. Freuling, Thomas Müller, Stefan Finke

Friedrich-Loeffler-Institut (FLI), Federal Research Institute for Animal Health, Institute of Molecular Virology and Cell Biology, 17493 Greifswald-Insel Riems, Germany

Corresponding author: stefan.finke@fli.de

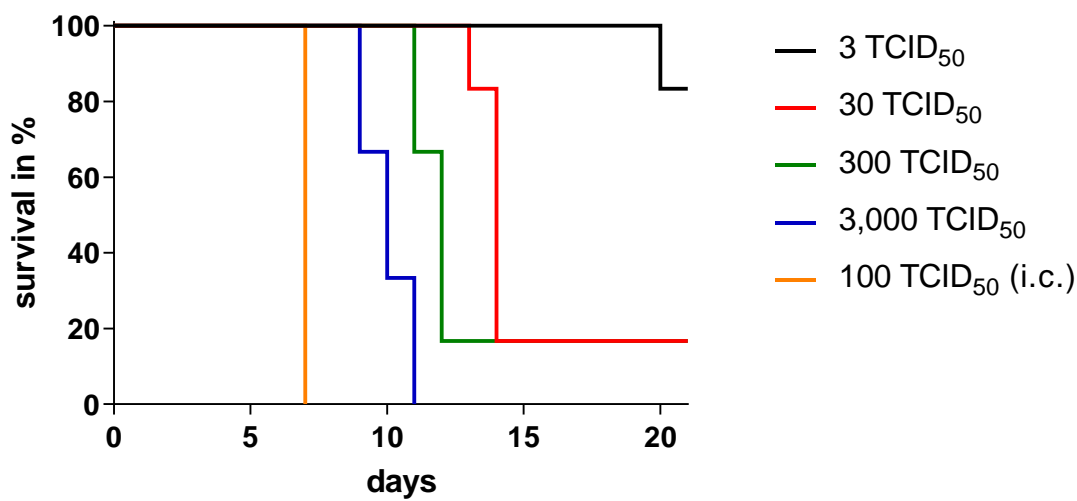


Fig. S1: Kaplan-Meier survival plot of RABV infection experiment. Comparison of dose-dependent survival of mice (six per group) after i.m. inoculation of rRABV Dog (3 to 3,000 TCID₅₀). A control group of three mice i.c.-inoculated with 100 TCID₅₀ rRABV Dog is shown in orange.

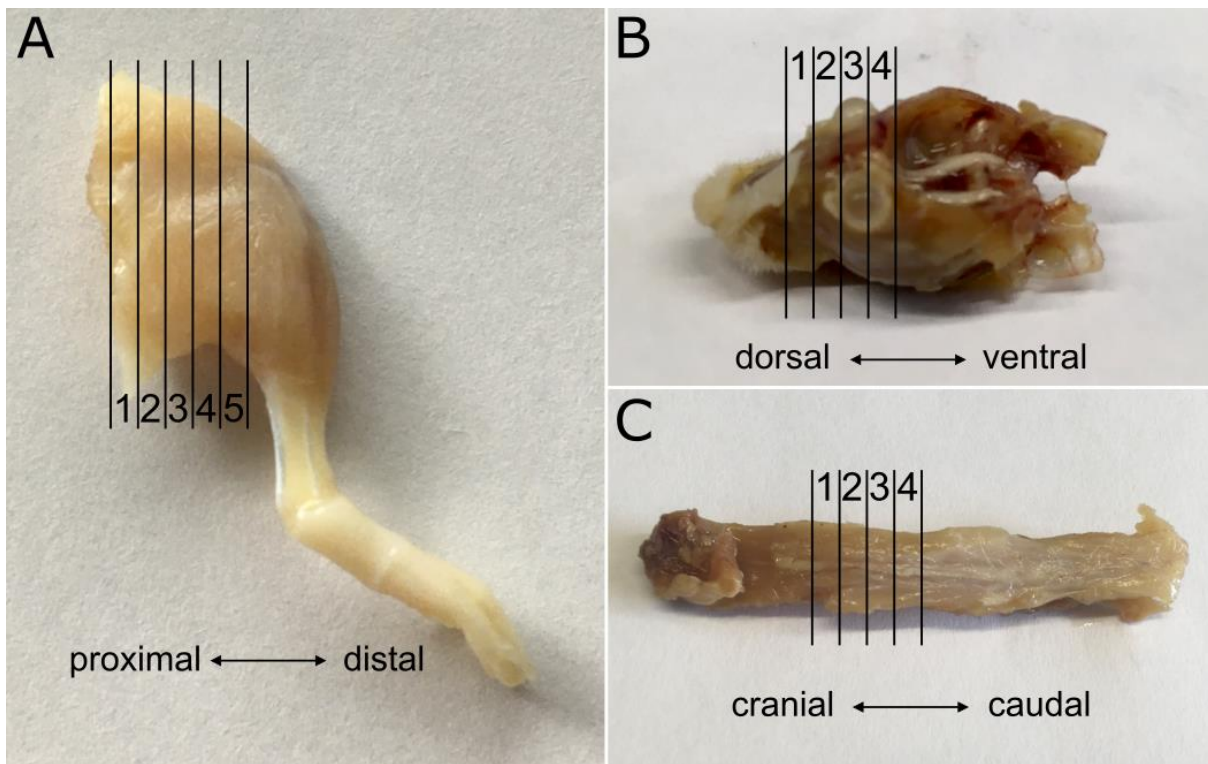


Fig. S2: Cutting pattern of cross-sections from peripheral tissues of infected mice. Hind legs (A), heads (B) and spinal columns (C) were decalcified and sectioned with a scalpel into several 1-2 mm thick slices.

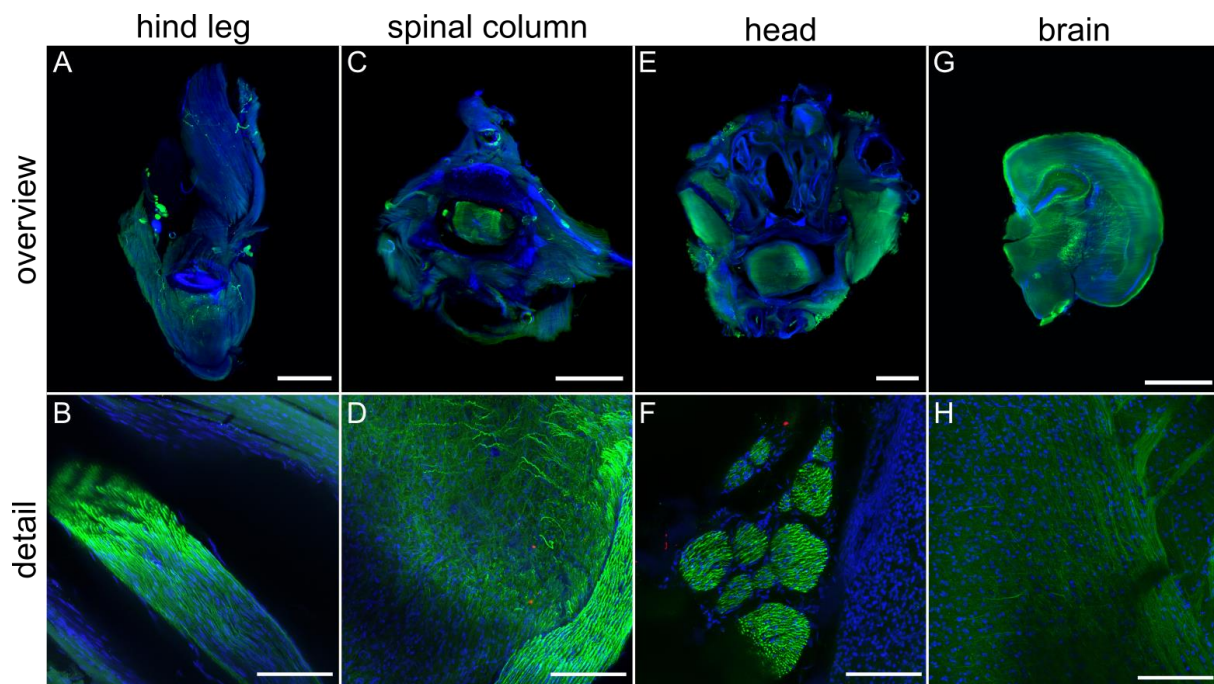


Fig. S3: Non-infected peripheral mouse tissues after indirect immunofluorescence staining against RV-P (red), NEFM (green) and nuclei (blue). Maximum z-projections of light sheet overviews and high-resolution confocal z-stacks from hind leg (A,B), spinal column (C,D), head (E,F) and brain (G,H). No RABV antigen was detected. Scale bar: 1,500 μm (overview), 100 μm (detail).

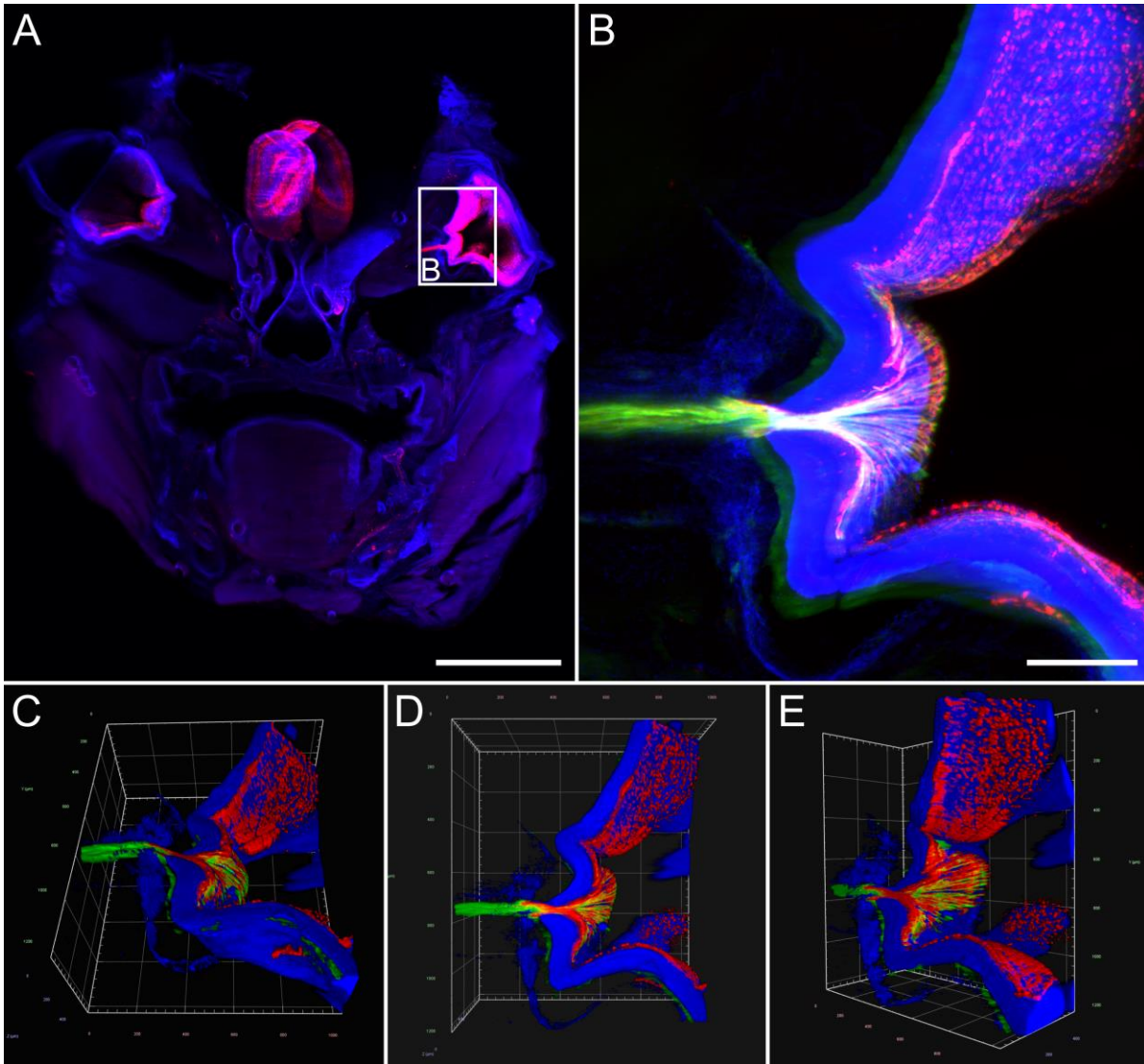


Fig. S4: Field RABV infection of optic nerve and retina. (A) Maximum z-projection of coronal mouse head section after i.c. inoculation [1.26x magnification, $z = 1,760 \mu\text{m}$, Scale bar $2,000 \mu\text{m}$]. RV-P (red), nuclei (blue). (B) Maximum z-projection of detail from (A) (see white box) with a magnification of 12.6x. Green: NEFM. Scale bar: $200 \mu\text{m}$. (C-E) Respective 3D projections of (B). Different viewing angles of the infection of the orbital cavity, including the optic nerve, are shown.

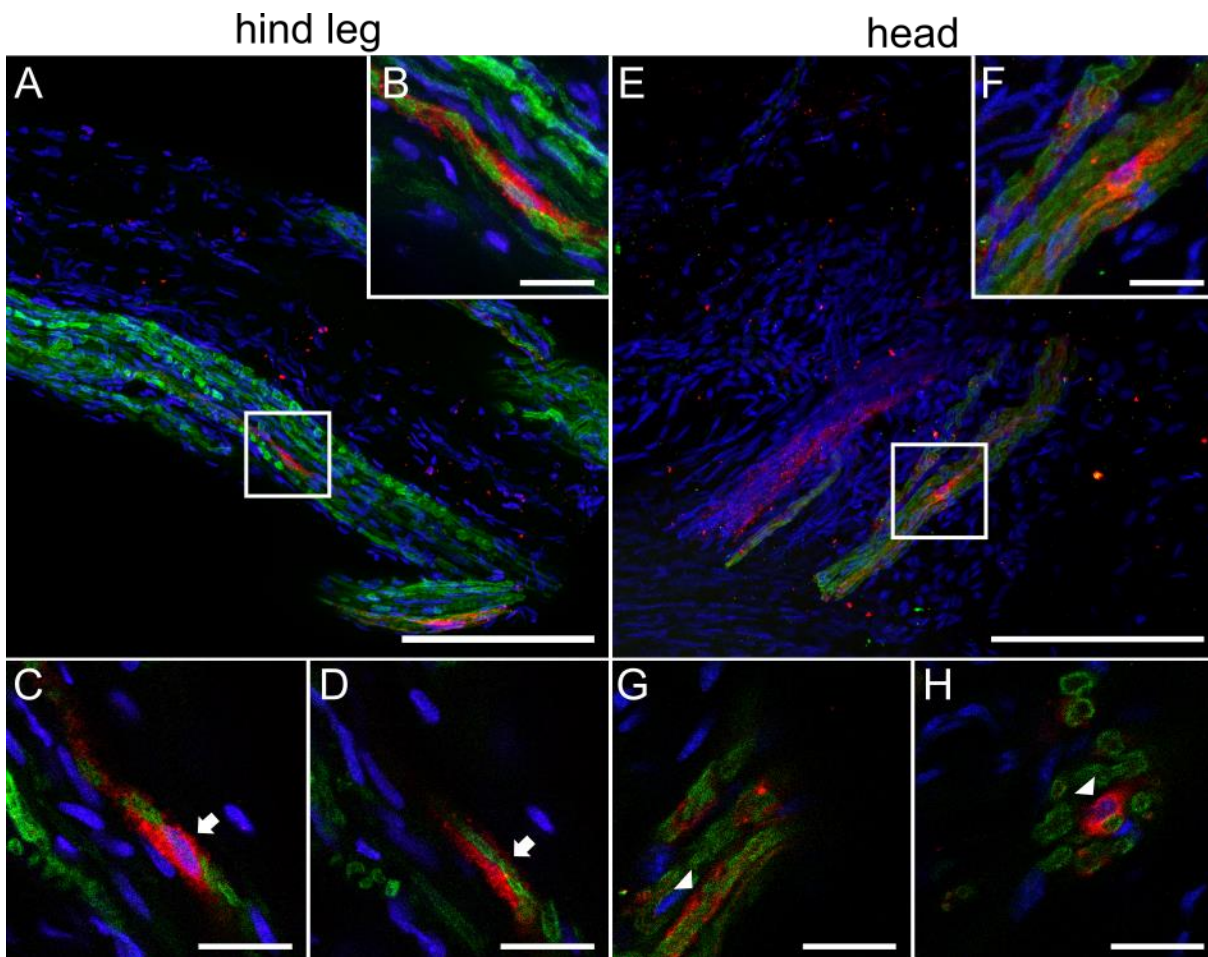


Fig. S5: A different, bat-associated field RABV demonstrates a comparable pattern of RABV P in hind leg and head nerves, including infected Schwann cells, after i.m. inoculation. (A,B) Maximum z-projection (A) and detail (B) of confocal high-resolution z-stacks of hind leg section from an i.m.-infected mice with RABV Bat [$z = 55 \mu\text{m}$; Scale bar: $100 \mu\text{m}$ (A), $15 \mu\text{m}$ (B)]. Indirect immunofluorescence staining against RABV P (red), MBP (green), and nuclei (blue). Individual infected nerve fibers were detected, in which RABV P surrounds the MBP signals. (C,D) Single planes of detail view from (B). RABV P was detected around MBP signals (white arrows). Scale bar: $15 \mu\text{m}$. (E,F) Maximum z-projection of nerve fibers in coronal head sections after i.m. inoculation of RABV Bat [$z = 31 \mu\text{m}$; Scale bar: $100 \mu\text{m}$ (A), $15 \mu\text{m}$ (B)]. Indirect immunofluorescence staining against RABV P (red), MBP (green) and nuclei (blue). (G,H) Single planes of detail view from (F). RABV P signals were located around MBP structures (white arrowheads). Scale bar: $15 \mu\text{m}$.

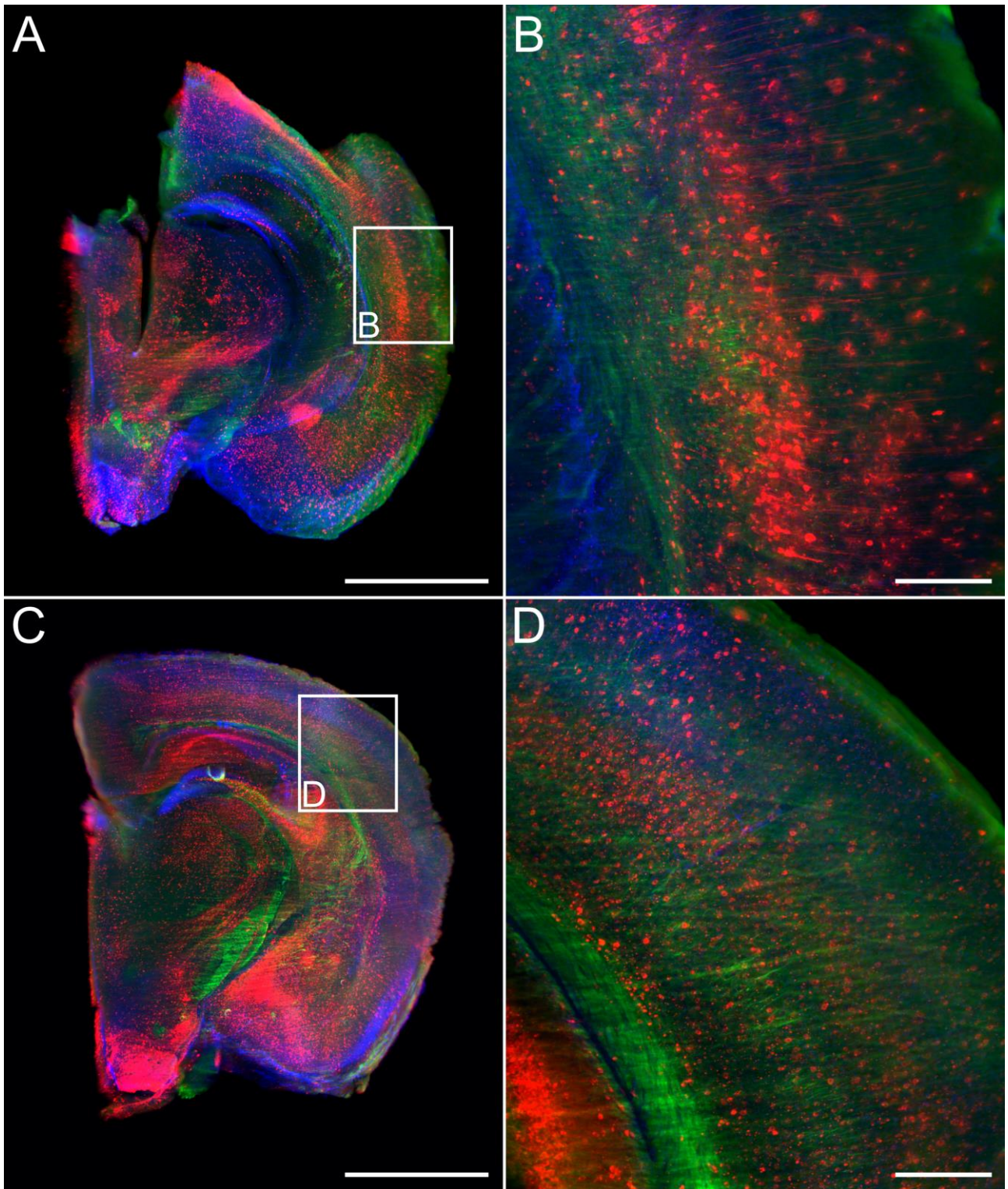


Fig. S6: Comparison of field RABV-infected brains after i.m. and i.c. inoculation in clinically diseased mice (10 and 7 days post-inoculation, respectively). (A,C) Independent of the inoculation route, the brains of i.m.- (A) and i.c. (C)-infected mice exhibited massive RABV infection throughout multiple areas of the brain, confirming strong CNS replication independent of the inoculation route. [2.5x magnification; [z = 1,282 μ m (A), 1,384 μ m (B)]. RABV P = red, NEFM = green, nuclei = blue. Scale bar: 1,500 μ m. (B,D) Maximum z-projection of details (white boxes) of A and C with magnification of [12.6x; z = 1,130 μ m (B), 386 μ m (D)]. Scale bar: 200 μ m.